

StarNet: Joint Action-Space Prediction with Star Graphs and Implicit Global Frame Self-Attention

Faris Janjoš¹, Maxim Dolgov¹, and J. Marius Zöllner²

Abstract—In this work, we present a novel multi-modal multi-agent trajectory prediction architecture, focusing on map and interaction modeling using graph representation. For the purposes of map modeling, we capture rich topological structure into vector-based star graphs, which enable an agent to directly attend to relevant regions along polylines that are used to represent the map. We denote this architecture StarNet, and integrate it in a single-agent prediction setting. As the main result, we extend this architecture to joint scene-level prediction, which produces multiple agents’ predictions simultaneously. The key idea in joint-StarNet is integrating the awareness of one agent in its own reference frame with how it is perceived from the points of view of other agents. We achieve this via masked self-attention. Both proposed architectures are built on top of the action-space prediction framework introduced in our previous work, which ensures kinematically feasible trajectory predictions. We evaluate the methods on the interaction-rich inD and INTERACTION datasets, with both StarNet and joint-StarNet achieving improvements over state of the art.

I. INTRODUCTION

Accurate prediction of the driving situation is a major cornerstone for achieving performant full autonomy of self-driving cars. Despite a strong research and industry focus, there are many problems to be solved, such as understanding complex social interactions among different agents and effectively incorporating rich topological information. Other important aspects are prediction of multi-modal trajectories, conditioning predictions on assumed goals of given agents, as well as achieving reasonable long-term predictions. In tackling these challenges, Deep Neural Networks (DNN) have shown great results over classical robotics approaches, especially for the use-case of urban driving.

The challenges of environment representation and interaction modeling are tightly coupled, e.g. the maneuvers of two negotiating vehicles in a highly-interactive situation are constrained by the road topology. Therefore, a learned model must consider the effects of topology on the driving situation. This makes the representation of map information paramount: it should enable explicitly relating to map elements such as lane centerlines and road boundaries, as well as segments along these elements. Furthermore, it must allow the model to discern between more and less important

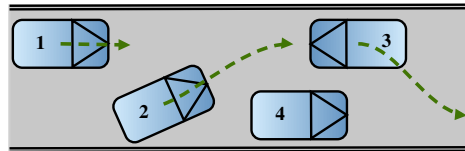


Fig. 1: Example of a highly interactive situation requiring joint scene prediction: vehicle 1 slows down to allow vehicle 2 to overtake parked vehicle 4; vehicle 3 must reverse behind vehicle 4.

segments. In this sense, a direct, explicit representation of map geometry serves to condition the social interaction.

Predictions for interacting vehicles in a driving scene must be consistent. Therefore, it is desirable to do a joint prediction and to consider mutual social interaction (example in Fig. 1). In contrast, predicting separately for each agent assumes that each vehicle considers others as part of its local environment. In this way, the scene at hand is considered from the point of view of each of the vehicles while marginalizing other vehicles, which is redundant and may lead to inconsistent predictions. This brings the question, how can we share this mutual local information? A potential solution is predicting jointly in a global reference frame; this eliminates the redundancy, but at the cost of an arbitrary dependency on the origin placement. Otherwise, performing individual, marginal predictions hinders sharing of intention information between local representations of the same agent.

In handling the joint nature of the prediction problem, many works use global representations centered around the autonomous vehicle (AV) [1], [2], [3], [4], [5], in the form of sensor data or generated Bird’s Eye View (BEV) images. In order to obtain agent-specific features, they extract patches around the agents of interest, derive corresponding latent information, and perform individual or joint predictions, provided that the latent features are combined. This introduces twofold disadvantages. First, grid-based environment representation assumes that the model extracts map objects and agents implicitly from individual pixels while inferring semantic knowledge. And second, the networks are tasked with associating information about the same agents from different sets of latent features, which might vary if the agents’ perspectives are different. In particular, if there is no overlap among the initial patches, it might be difficult to infer relational information between two agents if they don’t exist in each other’s immediate environment representations.

In our approach, we help our models learn by explicitly relating the same agents from other agents’ perspectives. Furthermore, we enable them to learn to attend to the most relevant map elements and their segments directly. The contributions of our work are the following:

¹ Robert Bosch GmbH, Corporate Research, Advanced Autonomous Systems, 71272 Renningen, Germany. {faris.janjos, maxim.dolgov}@de.bosch.com

² Research Center for Information Technology (FZI), 76131 Karlsruhe, Germany. zoellner@fzi.de

This work was financially supported by the Federal Ministry of Economic Affairs and Energy of Germany, grant number 19A20026H, based on a decision of the German Bundestag.

- A novel, star-graph-of-vectors polyline representation, with unconstrained field-of-view (given a map description) and direct modeling of most relevant segments.
- Joint scene-level prediction via self-attention [6], explicitly combining features from multiple reference frames while masking out irrelevant information.
- State-of-the-art performance on the INTERACTION dataset [7], containing challenging roundabout, intersection, and highway merge scenarios.

II. RELATED WORK

The field of trajectory prediction has generated an exhaustive literature [8]. Within the field of autonomous driving, the multifaceted nature of the problem yields works that focus on specific challenges within the overall landscape. They include but are not limited to: environment representation [9], [10], [11], multi-agent interaction [12], [13], [14], multi-modality [15], [16], [17], goal-conditioning [18], [19], [20], and kinematic constraints [21], [22], [23]. Furthermore, some works integrate prediction with detection and planning [24], [25], [3], as an important step in achieving end-to-end self-driving. Our work focuses on **map representation** and **interaction modeling**. In addressing these challenges, approaches using Convolutional Neural Networks (CNN) [26] and Graph Neural Networks (GNN) [27] are prevalent, with GNNs increasingly used over CNNs.

A. Graph-based map representation

Encoding map information into graphs and using GNNs offers several advantages over image-based inputs used in conjunction with CNNs. CNNs extract locational features from rasterized BEV images or grids with LiDAR point clouds. In contrast, GNNs can learn directly from graph-based representations, which encode the geometric structure of the road into nodes and edges. In doing so, they alleviate the need to infer objects from pixels, as well as improve efficiency due to fewer weights. Furthermore, graphs benefit from a larger field of view than rasters, which are usually restricted by image dimensions and resolution. These factors contribute to a substantially higher representation density.

VectorNet [9] is a seminal work that uses graph-based map representations. This approach fits polylines to map elements and dissects them into their constituent vectors. Then, fully-connected graphs are constructed per map element, which are aggregated by a GNN into a feature vector. This procedure is used as a basis in further works [16], [14], [17]. Alternative approaches are [10] and [28], redefining the graph convolution operation with additional adjacency matrices in order to capture a larger receptive field. Consequently, they are able to capture a longer range longitudinally, as well as account for the different semantic meaning of lateral lanes. Another class of works is [29] and [19], which model attention to specific lanes or sections along a reference polyline, constructed by concatenating individual polyline points. In the case of [19], this enables placement of hypothetical goals along the polyline to condition the trajectory prediction.

Works like VectorNet construct fully-connected subgraphs for each map element in order to mitigate the GNN information bottleneck¹ [30] problem. This enables each graph node to be no more than one hop away from any other node. However, as a result, unnecessary information is shared between vectors that are not physically close but are part of the same polyline. Thus, [9] only considers the nodes within a distance threshold to the predicted vehicle, in turn limiting the receptive field in aggregation. Another issue is that [9] includes ordering information into the node attributes via an integer index, which raises correctness questions since integers are combined with floating point features such as xy positions.

In our work, instead of connecting vectors by their polyline membership, we ask the question, which parts of a polyline are the most relevant *to an agent*? We task a Graph Attention Network (GAT) [31] with the answer; the attention mechanism learns to determine the most relevant vectors without artificially limiting the receptive field. Furthermore, our map representation is simpler to pre-process than [10], [28] since we use standard graph convolutions, as well as [19], [29], since we do not manually select the reference polyline and allow other map element types to be attended to as well.

B. Joint graph-based interaction modeling

Social interaction in a driving scene can inherently be represented as a natural graph, where nodes are agents and edges model their (weighted) connections. Hence, virtually all recent state-of-the-art approaches use graph-based learned models such as GNNs and Multi-Head Attention (MHA), which is related to the Transformer architecture² [6]. For the sake of brevity, we limit our review to joint prediction works [12], [18], [33], [2], [3], [4], [34], [35], [20], [5].

Among these approaches, [12], [18], [2], [3], [4], [34] use deep generative models. Here, they capture the uncertainty within a scene into a set of latent variables and sample from the latent space. The major drawback of such approaches is the randomness of their outputs because they require sampling from a latent distribution during inference. Thus, likelihood estimation of the predicted trajectory distribution is difficult. This is exacerbated in the single-step prediction approaches [12], [18], which construct a trajectory iteratively. Another drawback is limited map information; approaches either don't consider the map at all [33], or use global representations centered around the AV [2], [3], [4]. As mentioned in Sec. I, the AV-centered global view requires extracting local patches around each agent of interest and relating information implicitly via CNNs. As an alternative, [20] and [35] perform joint prediction in the global reference frame without AV-centering, but reduce the effects of arbitrary

¹Modeling the full map connectivity as a mesh-like natural graph and interweaving the agents nodes would result in long chains of propagated information. Learning over such a graph would necessitate many iterations of message passing and yield over-smoothed node embeddings.

²Incidentally, the basic Transformer layer is equivalent to the GNN GAT layer, in the case of multiple attention heads and a fully-connected underlying graph [32].

origin placement by injecting the global-frame map via cross-attention and Long Short-Term Memory (LSTM)-like [36] implicit gating, respectively.

In our work, we output deterministic predictions given deterministic inputs, as well as regressing one-shot trajectories. We model the map explicitly from graph-based representations with unlimited field of view. Our work is closest to the prediction model in [20], however, instead of using global reference frames, we ask the question, how is an agent jointly perceived by other agents? We arrive at a MHA model with masking, which combines multiple local representations to construct an implicit global frame. Furthermore, our model is smaller since it uses two GAT and two MHA layers to model the map and social interaction, compared to 18 MHA layers in [20]. Finally, we frame our model in the action-space framework introduced in our previous work [23], ensuring kinematically feasible predictions.

III. METHOD

A. Background

Consider the task of vehicle trajectory prediction in a driving situation with N heterogeneous interacting agents. We define the single-agent prediction problem as predicting the distribution of future waypoints \hat{Y}_i of vehicle i . It can be framed in an imitation learning setting, where a learned model parameterizes the distribution

$$\hat{Y}_i \sim P(\hat{Y}_i | \mathcal{D}^i), \quad (1)$$

conditioned on the local context \mathcal{D}^i of vehicle i . Here, the superscript indicates that the values are represented in the local reference frame of vehicle i , subscript indicates prediction for agent i , while $\hat{\cdot}$ denotes predicted future values. We simplify the problem in (1) by predicting a sample \hat{Y}_i of the distribution, e.g. a $2 \times T$ matrix of xy coordinates over T future time steps.

The context $\mathcal{D}^i = \{\mathcal{M}^i, \mathcal{T}^i\}$ contains the map \mathcal{M}^i and past position tracks \mathcal{T}^i of vehicle i and its neighboring $N-1$ agents, with $\mathcal{T}^i = \{X_j^i\}_{j=1}^N$. Each track X_j^i is a $3 \times T$ matrix of xy coordinates of agent j over T past time steps (in the reference frame of vehicle i at the current time step) and a padding row, since the agent might not be present in the scene for each time step. The padding row contains zeros for non-existent points (and zero positions) and ones otherwise.

In joint prediction, we consider the task of predicting K ($K \leq N$) vehicles' trajectories simultaneously. Thus, the learned model parameterizes the distribution

$$\hat{Y} \sim P(\hat{Y} | \mathcal{D}). \quad (2)$$

Therefore, we predict a sample \hat{Y} of \hat{Y} for future trajectories of all K vehicles, given their contexts \mathcal{D} , where $\hat{Y} = \{\hat{Y}_k\}_{k=1}^K$ and $\mathcal{D} = \{\mathcal{D}^k\}_{k=1}^K$, respectively. Each \mathcal{D}^k can be separated into its map and tracks components, \mathcal{M}^k and $\mathcal{T}^k = \{X_j^k\}_{j=1}^N$. Note that tracks \mathcal{T}^k contain trajectories for all N agents, including those whose waypoints are not predicted such as pedestrians and bicycles.

In parameterizing the distributions in (1) and (2), we use a general encoder–decoder structure, with a context encoder

and an output decoder. The encoder reasons about the context \mathcal{D} while the decoder generates predicted trajectories \hat{Y} . Furthermore, we make use of track encoders, e.g. we encode each agent track X_j^i ($i \in [1, \dots, K]$, $j \in [1, \dots, N]$) into a feature vector z_j^i via a 1D CNN network.

B. Action-space prediction

We use positional representations in modeling the environment \mathcal{D} within the context encoder. Both the polyline map \mathcal{M} (as will be shown later), as well as the tracks \mathcal{T} , contain xy coordinates describing polyline control points and past trajectories, respectively. Hence, in generating learned feature representations of the environment, map-dependent interactions are inferred from data in the Euclidean space.

However, when generating the predicted trajectories \hat{Y} via the decoder, we shift the learning problem into the action-space of accelerations and steering angles. We provide past actions as action tracks A_i^i ($i \in [1, \dots, K]$) and generate future actions with a Gated Recurrent Unit (GRU) [37]. This is consistent with the action-space prediction framework [23] and guarantees that a learned model does not have to capture motion models, as well as ensuring kinematic feasibility (with an output kinematic model). Similarly to position tracks, we encode past action tracks A_i^i into feature vectors w_i^i with the same network.

C. Single-agent prediction with StarNet

In this section, we present a single-agent prediction method for regressing the future trajectory of vehicle i (prediction-ego). We approximate (1) via a deterministic encoder–decoder model. The encoder consists of a star graph map model and a map-dependent interaction model, while the decoder is a multi-modal action predictor, directly generating m samples from the distribution (1).

1) *Star graph map model*: Key component of single-agent StarNet is its representation of map elements via star graphs. First, each map element, such as a sidewalk, lane center-line, or a traffic island, is approximated by a polyline consisting of fixed-length vectors, similarly as in VectorNet [9]. Thus, the representation \mathcal{M}^i of the map in the agent i 's reference frame consists of Q polylines

$$\mathcal{M}^i = \{q_j^i\}_{j=1}^Q. \quad (3)$$

In turn, each polyline consists of L vectors comprising their start and end xy coordinates and one-hot type encoding

$$q_j^i = \{v_{jl}^i\}_{l=1}^L, \quad (4)$$

$$v_{jl}^i = [v_{\text{start}}, v_{\text{end}}, v_{\text{type}}]^T. \quad (5)$$

Given this polyline representation, we construct a directed star graph for each polyline q_j^i . In this structure, the past prediction-ego track is the central node with embedded track features z_i^i and edges connecting each vector v_{jl}^i to the central node. To ensure message passing compatibility, we embed the vector nodes (5) into the same dimensionality as the features z_i^i using a linear layer. Finally, we feed this graph to a 2-layer GAT and aggregate the nodes via max-pooling to obtain polyline-level embeddings q_j^i of same dimensionality as the nodes. This structure is depicted in Fig. 2.

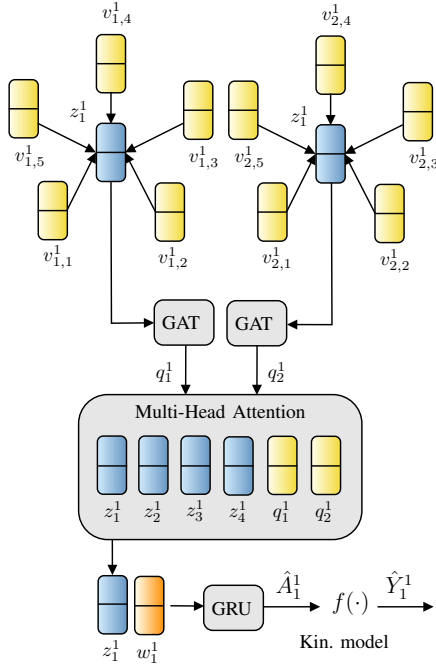
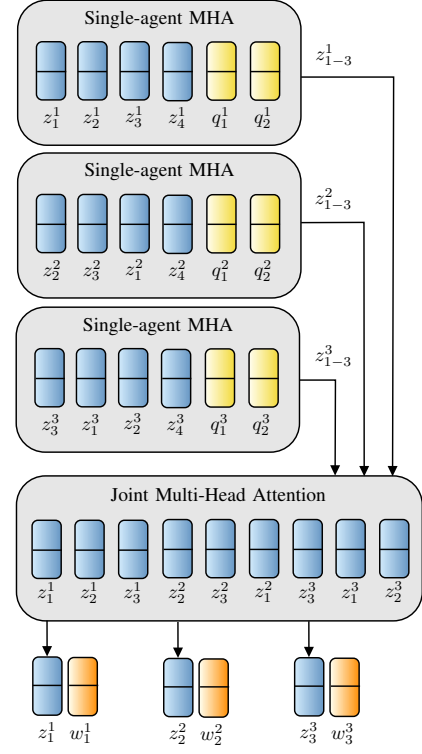


Fig. 2: StarNet single-agent architecture for the driving scene in Fig. 1. Vehicle 1 is the prediction-ego, and two polylines and three neighboring agents are in its local context. First, the two polylines determined by five vectors each are represented in a directed star graph with prediction-ego track embedding z_1^1 in the center and vector embeddings $v_{\{1,2\},\{1,5\}}^1$ outward. Polyline-level embeddings are generated by a 2-layer GAT, followed by a 1-layer Multi-Head Attention modeling map-dependent social interaction via aggregating all agents’ and polylines’ embeddings, $z_{\{1,4\}}^1$ and $q_{\{1,2\}}^1$ respectively. Then, prediction-ego embedding is selected, concatenated with its action track embedding w_1^1 , and fed through an action-prediction GRU to predict future actions \hat{a}_1^1 . Finally, positions \hat{x}_1^1 are obtained via a kinematic model transformation.

The star graph and the accompanying GAT model the relationship between the ego track and the map. Contrary to VectorNet’s fully-connected graphs, we assume that there is more information contained in the vehicle’s direct attention (represented by its past track embedding) to a specific vector within a polyline rather than between the polyline vectors themselves. This allows us to expand the receptive field, since the attention mechanism will learn to ignore distant vectors, and to consider them proportionally to their weights in aggregation. Furthermore, the structure removes the need to include artificial ordering into the vector (5), as it is done in VectorNet in order to help convey the polyline geometry, which simplifies the learning problem.

2) *Map-dependent interaction model*: In the single-agent StarNet, we model map-dependent social interaction with a MHA [6], see Fig. 2. We combine vehicle i ’s past track embedding z_i^i with polyline embeddings q_j^i ($j \in [1, \dots, Q]$), as well as track embeddings z_j^i ($j \in [1, \dots, N - 1]$) of each agent sharing the scene with i . Then, we stack the embedding vectors into a matrix with $N + Q$ rows and feed it into a single MHA layer. Here, linear projections of the input are generated in the form of query, key, and value matrices. Then, the self-attention operation [6] is applied in order to infer the relationships between the embeddings. The



(a) Joint-StarNet with both map element star-graphs and action decoder blocks omitted: Single-agent Multi-Head Attention blocks model local map-dependent social interaction for the joint prediction candidate vehicles 1 – 3. Features z_{1-3}^1 , z_{1-3}^2 , z_{1-3}^3 are selected and fed into the Joint Multi-Head Attention block, which aggregates local features to construct an implicit global frame. After this operation, features z_i^i ($i \in [1, 2, 3]$) are selected and together with their action embeddings w_i^i fed into the action decoder block (not shown).

1	0	0	0	0	1	0	1	0
0	2	0	2	0	0	0	0	2
0	0	3	0	3	0	3	0	0
1	0	0	0	0	1	0	1	0
0	2	0	2	0	0	0	0	2
0	0	3	0	3	0	3	0	0
1	0	0	0	0	1	0	1	0
0	2	0	2	0	0	0	0	2
0	0	3	0	3	0	3	0	0

(b) Depicted is the corresponding 9×9 attention mask matrix for the three vehicles from Fig 3a. Here, each non-zero number denotes attention to a feature vector of a vehicle in a row, while zero denotes no attention. Each 3×3 matrix in a block-row can be obtained by left-shifting the left-neighbor 3×3 matrix by one.

Fig. 3: Joint-StarNet architecture in Fig. 3a (for the scene in Fig. 2) and the accompanying attention mask for the Joint Multi-Head Attention block in Fig. 3b.

output of the MHA is of the same dimensionality as the stacked input matrix, and we select the row that corresponds to the vehicle i . Through the GAT and MHA layers, the obtained embedding is able to capture the map-dependent social interaction in the local context of the prediction-ego. The next step is feeding it into the action output decoder.

3) *Multi-modal action decoder*: The action decoder combines the positional embedding of the prediction-ego, aggregated to consider the map-dependent social interaction, with its action embedding. We concatenate z_i^i with w_i^i and feed it into the action decoder, which is the same GRU network as in [23] (depicted in Fig. 2). It generates steering angles and accelerations, directly predicting m action modes

(trajectories and softmax scores, which can be interpreted as probabilities), similarly to [38]. Then, a bicycle kinematic model converts actions to future positions.

We train the whole pipeline with the loss

$$\mathcal{L} = \mathcal{L}_{\text{reg}} + \beta \mathcal{L}_{\text{class}}, \quad (6)$$

where \mathcal{L}_{reg} considers the mismatch to the ground-truth future trajectory and $\mathcal{L}_{\text{class}}$ considers the mode probability via cross-entropy, same as in [23], with β set to 1.

D. Joint prediction with joint-StarNet

In this section, we present a joint prediction method for regressing the future trajectory of k vehicles in a driving scene ($k \in [1, \dots, K], K \leq N$). We directly model the joint distribution (2) without factorizing individual agents. The joint-StarNet architecture builds on StarNet from Sec. III-C and achieves joint prediction by aggregating local features into an implicit global frame via masked self-attention.

1) *Implicit global frame self-attention*: The joint-StarNet is an extension to single-agent StarNet. After determining the joint prediction candidates, we perform the first two steps of the single-agent StarNet pipeline separately for each vehicle. We construct local map element star graphs, aggregate them with GATs and combine them with locally embedded tracks in the Single-Agent MHA blocks. Then, we select the positional embeddings corresponding to each of the joint agents, in each joint agent’s local context, obtaining K^2 feature vectors $\{\{z_j^k\}_{j=1}^K\}_{k=1}^K$. An example is provided in Fig. 3a. This combination of features contains mutual local information about each joint prediction candidate, at the cost of quadratically increasing number of features. Nevertheless, we do not observe a computational bottleneck due to efficient batching in training, described in Sec. IV-A.

Given the individual local features, we now construct an implicit global frame by combining features from each local frame. We achieve this with another MHA block (denoted as Joint Multi-Head Attention in Fig. 3a), taking in features $\{\{z_j^k\}_{j=1}^K\}_{k=1}^K$ stacked into a matrix. In the output, we select the rows corresponding to features $\{z_k^k\}_{k=1}^K$ (in their respective reference frames) and feed them in a batched manner into an action decoder block. We can train with the same loss (6) as in single-agent StarNet training.

2) *Attention-mask*: In combining multiple local contexts into an implicit global context, the embeddings corresponding to a single vehicle in different local frames should attend only to themselves. We achieve this by limiting the self-attention with a $K^2 \times K^2$ attention mask matrix. It ensures that only the features $\{z_j^k\}_{k=1}^K$ for the agent j in different frames are considered, in each row of the stacked input matrix. This is exemplified in Fig. 3b.

The joint-StarNet architecture with masking allows to explicitly combine multiple local interaction models and integrate them into an implicit global interaction model. Each local, single-agent model uses direct map representations that condition the local social interaction. Furthermore, predictions are generated with an action-space learned model that fully captures kinematic characteristics of motion.

	inD [39]		INTERACTION [7]	
	ADE	FDE	ADE	FDE
FFW-ASP [23]	0.37	1.02	0.24	0.63
VectorNet [9]	0.37	1.03	0.22	0.63
StarNet	0.35	0.98	0.16	0.49
joint-StarNet	0.32	0.89	0.14	0.41

TABLE I: Comparison of StarNet and joint-StarNet with FFW-ASP [23] and VectorNet [9] (own implementation).

	INTERACTION [7]	
	ADE	FDE
DESIRE [40]	0.32	0.88
MultiPath [15]	0.30	0.99
STG-DAT [34]	0.29	0.54
TNT [16]	0.21	0.67
ReCoG [41]	0.19	0.66
HEAT-I-R [35]	0.19	0.65
ITRA [5]	0.17	0.49
StarNet	0.16	0.49
joint-StarNet	0.14	0.41

TABLE II: Comparison of StarNet and joint-StarNet with approaches in literature (reported results). The values for [40] and [15] are given in [16]. Since [34] reports results for different map types separately, we computed the aggregate value by combining the ratios of specific map types in the validation dataset.

IV. RESULTS

A. Implementation

For implementing the StarNet (Sec. III-C) and joint-StarNet (Sec. III-D) architectures we used several network types: 1D CNNs, GATs, MHA, and GRUs. The track encoder 1D CNNs are adapted from the ActorNet model in [10] and embed position and action tracks to 128- and 64-dimensional vectors, respectively. The position embeddings are then used as nodes in the GAT and MHA networks, which are both realized with 8 attention heads. In the action decoder block, the concatenated position and action track embeddings are first transformed by two linear layers of sizes $\{512, 256\}$ (with batch normalization and \tanh activation) before being fed into the GRU network. The GRU iterates these transformed features three times through two layers of 512 hidden units, directly predicting m future action modes.

The joint-StarNet has several important practical considerations. Within the model, each joint candidate is first fed through the first two steps of the single-agent StarNet (Sec. III-C.1 and Sec. III-C.2), and then the features from multiple local contexts are aggregated in the Joint MHA, as exemplified in Fig. 3a. In a single batch element, this induces linearly growing complexity in the GAT and Single-agent MHA and quadratically growing complexity in the Joint MHA, with the number of joint candidates. However, the computational load does not grow equally due to efficient batching of different scenes. In the GAT case, we aggregate different star graphs into a single graph with a block-diagonal adjacency matrix. Similarly, in both MHA blocks we feed inputs from different scenes together in a batch, but use additional batch-wise attention mask. As a result, this brings a higher utilization of GPU memory. However, reasonably-sized batches are made possible by the compact input representations.

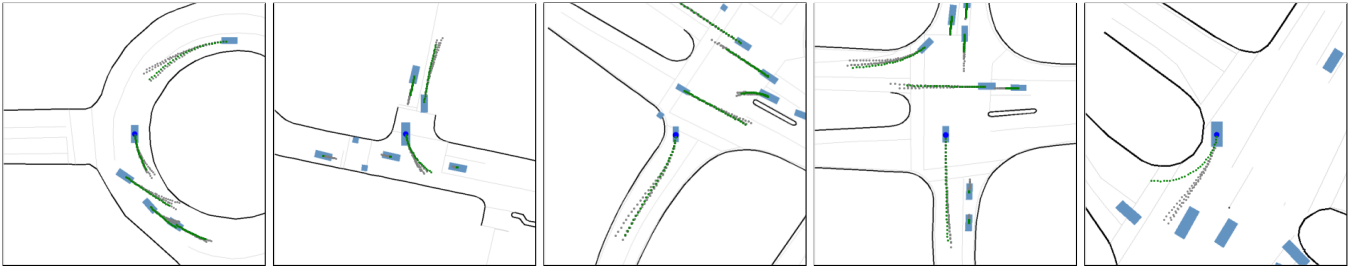


Fig. 4: Qualitative results of joint-StarNet on INTERACTION [7] validation subset. Rectangles indicate vehicles, while squares are pedestrians/bicycles. Gray trajectories are predictions ($m = 3$ modes), with the ground truth overlaid in green. The right-most prediction is among the 50 worst individual predictions according to the FDE metric.

B. Datasets

Datasets must allow flexibility in choosing single or multiple prediction targets, in order to facilitate both single-agent and joint trajectory prediction. Therefore, we selected the inD [39] and the INTERACTION datasets [7] that provide joint tracked data over a whole recording. In both datasets, we generated individual samples for all agents except pedestrians and bicycles by extracting all 2.5+3s segments (2.5s past and 3s prediction recorded with 10Hz) with a 1.5s spacing between the samples. In generating map data, we used the provided lanelets [42] to extract two polyline types: road boundaries (e.g. curbstones) and road properties (e.g. lane center-lines). For inD, we used the same training/validation/testing split as in [23], and for INTERACTION we used the provided validation dataset.

In the joint-StarNet setting, it is non-trivial to determine the joint prediction candidates. We perform this by first selecting one vehicle in the scene that is present over an entire prediction time interval as the virtual-ego. Then, we determine all other vehicles that exist throughout the time interval and that at any time during the interval come close to the virtual-ego within a certain threshold; better approaches to filter relevant agents are left for future work. In this sense, the virtual-ego mimics an AV that predicts trajectories of its nearby vehicles (and its own trajectory). Thus, when another vehicle is chosen to be the virtual-ego, a different set of joint candidates could emerge. This allows us to effectively upsample highly interactive training data.

C. Training setup

We implemented our models in PyTorch [43] and trained with the Adam optimizer [44] over 10 epochs with batch size 8. The learning rate was set to 10^{-4} and multiplied by 0.2 for every two consecutive epochs with no improvement outside an ϵ region. In the joint-StarNet case, the training took around five days to complete on a single NVIDIA GeForce RTX 3090.

D. Performance

We compared our approaches against the raster-based Feed-Forward Action-Space Prediction (FFW-ASP) architecture from our previous work [23] and our own implementation of VectorNet [9], with the results shown in Tab. I. To ensure a fair comparison, we used our multi-modal action output decoder in VectorNet (originally uni-modal)

and did not incorporate the self-supervised map completion task from [9] within the MHA blocks of any architecture. Similarly, we adapted the FFW-ASP to use action track encoders mentioned in Sec. III-B. In all architectures, we set the number of predicted modes m to 3. As metrics, we computed the Average Displacement Error (ADE) and Final Displacement Error (FDE), defined as in [5].

As seen in Tab. I, StarNet’s graph-based map modeling and map-conditioned interaction modeling already brings improvements over the baseline methods. Similarly, joint-StarNet improves on StarNet’s performance, as expected. We also compared against reported results in literature on the INTERACTION validation dataset, see Tab. II. To the best of our knowledge, joint-StarNet achieves state-of-the-art performance.

Examples of predicted trajectories with joint-StarNet are shown in Fig. 4. It can be seen that overall the predictions accurately model the interaction in a scene. Regarding multi-modality, we observe that in most cases the modes are distributed realistically, i.e. in straight driving they are spread longitudinally and slight turns result in relatively narrow dispersion. However, among the shown worst prediction example, turns with a larger radius result in occasional missed modes, indicating room for improvement.

V. CONCLUSION

In this work, we presented an attention-based approach to directly represent map elements and explicitly model mutual social interaction. We offered two novel architectures, the single-agent StarNet that models map elements as star graphs, and a joint prediction extension via an additional MHA layer. The joint-StarNet can handle a variable number of agents and integrate their local awarenesses into an implicit global model. In this sense, it contributes an important step towards joint scene understanding.

In future work, we will focus on the multi-modality aspect of joint prediction and address the shortcomings mentioned in Sec. IV-D. We plan to improve on the implicit modeling of multi-modality within the action output decoder, which does not condition predicted modes on other vehicles’ predicted modes. Furthermore, we plan to integrate the presented architectures with the self-supervised long-term prediction framework of [23], which predicts future context representations prior to trajectories. We expect that the denser map and joint interaction modeling will lead to improved context prediction, bringing further performance improvements.

REFERENCES

- [1] S. Casas, C. Gulino, R. Liao, and R. Urtasun, "SPAGNN: Spatially-Aware Graph Neural Networks for Relational Behavior Forecasting from Sensor Data," in *2020 IEEE International Conference on Robotics and Automation (ICRA)*. IEEE, 2020.
- [2] S. Casas, C. Gulino, S. Suo, K. Luo, R. Liao, and R. Urtasun, "Implicit Latent Variable Model for Scene-Consistent Motion Forecasting," *arXiv preprint arXiv:2007.12036*, 2020.
- [3] A. Cui, A. Sadat, S. Casas, R. Liao, and R. Urtasun, "LookOut: Diverse Multi-Future Prediction and Planning for Self-Driving," *arXiv preprint arXiv:2101.06547*, 2021.
- [4] S. Suo, S. Regalado, S. Casas, and R. Urtasun, "TrafficSim: Learning to Simulate Realistic Multi-Agent Behaviors," in *Proceedings of the IEEE/CVF Conference on Computer Vision and Pattern Recognition*, 2021.
- [5] A. Scibior, V. Lioutas, D. Reda, P. Bateni, and F. Wood, "Imagining The Road Ahead: Multi-Agent Trajectory Prediction via Differentiable Simulation," *arXiv preprint arXiv:2104.11212*, 2021.
- [6] A. Vaswani, N. Shazeer, N. Parmar, J. Uszkoreit, L. Jones, A. N. Gomez, Ł. Kaiser, and I. Polosukhin, "Attention Is All You Need," in *Advances in Neural Information Processing Systems*, 2017.
- [7] W. Zhan, L. Sun, D. Wang, H. Shi, A. Clausse, M. Naumann, J. Kummerle, H. Konigshof, C. Stiller, A. de La Fortelle *et al.*, "INTERACTION Dataset: An INTERnational, Adversarial and Cooperative MOTION Dataset in Interactive Driving Scenarios with Semantic Maps," *arXiv preprint arXiv:1910.03088*, 2019.
- [8] A. Rudenko, L. Palmieri, M. Herman, K. M. Kitani, D. M. Gavrila, and K. O. Arras, "Human Motion Trajectory Prediction: A Survey," *The International Journal of Robotics Research*, vol. 39, no. 8, 2020.
- [9] J. Gao, C. Sun, H. Zhao, Y. Shen, D. Anguelov, C. Li, and C. Schmid, "VectorNet: Encoding HD Maps and Agent Dynamics from Vectorized Representation," in *Proceedings of the IEEE/CVF Conference on Computer Vision and Pattern Recognition*, 2020.
- [10] M. Liang, B. Yang, R. Hu, Y. Chen, R. Liao, S. Feng, and R. Urtasun, "Learning Lane Graph Representations for Motion Forecasting," in *European Conference on Computer Vision*. Springer, 2020.
- [11] Y. Hu, W. Zhan, and M. Tomizuka, "Scenario-Transferable Semantic Graph Reasoning for Interaction-Aware Probabilistic Prediction," *arXiv preprint arXiv:2004.03053*, 2020.
- [12] C. Tang and R. R. Salakhutdinov, "Multiple Futures Prediction," in *Advances in Neural Information Processing Systems*, 2019.
- [13] J. Li, F. Yang, H. Ma, S. Malla, M. Tomizuka, and C. Choi, "RAIN: Reinforced Hybrid Attention Inference Network for Motion Forecasting," *arXiv preprint arXiv:2108.01316*, 2021.
- [14] E. Tolstaya, R. Mahjourian, C. Downey, B. Vadarajan, B. Sapp, and D. Anguelov, "Identifying Driver Interactions via Conditional Behavior Prediction," *arXiv preprint arXiv:2104.09959*, 2021.
- [15] Y. Chai, B. Sapp, M. Bansal, and D. Anguelov, "MultiPath: Multiple Probabilistic Anchor Trajectory Hypotheses for Behavior Prediction," *arXiv preprint arXiv:1910.05449*, 2019.
- [16] H. Zhao, J. Gao, T. Lan, C. Sun, B. Sapp, B. Vadarajan, Y. Shen, Y. Shen, Y. Chai, C. Schmid *et al.*, "TNT: Target-driveN Trajectory Prediction," *arXiv preprint arXiv:2008.08294*, 2020.
- [17] Y. Liu, J. Zhang, L. Fang, Q. Jiang, and B. Zhou, "Multimodal Motion Prediction with Stacked Transformers," in *Proceedings of the IEEE/CVF Conference on Computer Vision and Pattern Recognition*, 2021.
- [18] N. Rhinehart, R. McAllister, K. Kitani, and S. Levine, "PRECOG: Prediction Conditioned on Goals in Visual Multi-Agent Settings," in *Proceedings of the IEEE International Conference on Computer Vision*, 2019.
- [19] S. Khandelwal, W. Qi, J. Singh, A. Hartnett, and D. Ramanan, "What-If Motion Prediction for Autonomous Driving," *arXiv preprint arXiv:2008.10587*, 2020.
- [20] J. Ngiam, B. Caine, V. Vasudevan, Z. Zhang, H.-T. L. Chiang, J. Ling, R. Roelofs, A. Bewley, C. Liu, A. Venugopal *et al.*, "Scene Transformer: A Unified Multi-Task Model for Behavior Prediction and Planning," *arXiv preprint arXiv:2106.08417*, 2021.
- [21] H. Cui, T. Nguyen, F.-C. Chou, T.-H. Lin, J. Schneider, D. Bradley, and N. Djuric, "Deep Kinematic Models for Physically Realistic Prediction of Vehicle Trajectories," *arXiv preprint arXiv:1908.00219*, 2019.
- [22] T. Phan-Minh, E. C. Grigore, F. A. Boulton, O. Beijbom, and E. M. Wolff, "CoverNet: Multimodal Behavior Prediction Using Trajectory Sets," in *Proceedings of the IEEE/CVF Conference on Computer Vision and Pattern Recognition*, 2020.
- [23] F. Janjoš, M. Dolgov, and M. J. Zöllner, "Self-Supervised Action-Space Prediction for Automated Driving," in *2021 IEEE Intelligent Vehicles Symposium (IV)*. IEEE, 2021.
- [24] W. Zeng, W. Luo, S. Suo, A. Sadat, B. Yang, S. Casas, and R. Urtasun, "End-to-End Interpretable Neural Motion Planner," in *Proceedings of the IEEE/CVF Conference on Computer Vision and Pattern Recognition*, 2019.
- [25] W. Zeng, S. Wang, R. Liao, Y. Chen, B. Yang, and R. Urtasun, "DSD-Net: Deep Structured Self-Driving Network," in *European Conference on Computer Vision*. Springer, 2020.
- [26] Y. LeCun, Y. Bengio, and G. Hinton, "Deep Learning," *Nature*, vol. 521, no. 7553, 2015.
- [27] Z. Wu, S. Pan, F. Chen, G. Long, C. Zhang, and S. Y. Philip, "A Comprehensive Survey on Graph Neural Networks," *IEEE transactions on neural networks and learning systems*, vol. 32, no. 1, 2020.
- [28] W. Zeng, M. Liang, R. Liao, and R. Urtasun, "LaneRCNN: Distributed Representations for Graph-Centric Motion Forecasting," *arXiv preprint arXiv:2101.06653*, 2021.
- [29] J. Pan, H. Sun, K. Xu, Y. Jiang, X. Xiao, J. Hu, and J. Miao, "Lane-Attention: Predicting Vehicles' Moving Trajectories by Learning Their Attention Over Lanes," in *2020 IEEE/RSJ International Conference on Intelligent Robots and Systems (IROS)*. IEEE, 2020.
- [30] U. Alon and E. Yahav, "On the Bottleneck of Graph Neural Networks and its Practical Implications," *arXiv preprint arXiv:2006.05205*, 2020.
- [31] P. Veličković, G. Cucurull, A. Casanova, A. Romero, P. Lio, and Y. Bengio, "Graph Attention Networks," *arXiv preprint arXiv:1710.10903*, 2017.
- [32] W. L. Hamilton, "Graph Representation Learning," *Synthesis Lectures on Artificial Intelligence and Machine Learning*, vol. 14, no. 3, 2020.
- [33] J. Mercat, T. Gilles, N. El Zoghby, G. Sandou, D. Beauvois, and G. P. Gil, "Multi-Head Attention for Multi-Modal Joint Vehicle Motion Forecasting," in *2020 IEEE International Conference on Robotics and Automation (ICRA)*. IEEE, 2020.
- [34] J. Li, H. Ma, Z. Zhang, J. Li, and M. Tomizuka, "Spatio-Temporal Graph Dual-Attention Network for Multi-Agent Prediction and Tracking," *arXiv preprint arXiv:2102.09117*, 2021.
- [35] X. Mo, Y. Xing, and C. Lv, "Heterogeneous Edge-Enhanced Graph Attention Network For Multi-Agent Trajectory Prediction," *arXiv preprint arXiv:2106.07161*, 2021.
- [36] S. Hochreiter and J. Schmidhuber, "Long Short-Term Memory," *Neural computation*, vol. 9, no. 8, 1997.
- [37] K. Cho, B. Van Merriënboer, C. Gulcehre, D. Bahdanau, F. Bougares, H. Schwenk, and Y. Bengio, "Learning Phrase Representations Using RNN Encoder-Decoder for Statistical Machine Translation," *arXiv preprint arXiv:1406.1078*, 2014.
- [38] H. Cui, V. Radosavljevic, F.-C. Chou, T.-H. Lin, T. Nguyen, T.-K. Huang, J. Schneider, and N. Djuric, "Multimodal Trajectory Predictions for Autonomous Driving Using Deep Convolutional Networks," in *2019 International Conference on Robotics and Automation (ICRA)*. IEEE, 2019.
- [39] J. Bock, R. Krajewski, T. Moers, S. Runde, L. Vater, and L. Eckstein, "The inD Dataset: A Drone Dataset of Naturalistic Road User Trajectories at German Intersections," *arXiv preprint arXiv:1911.07602*, 2019.
- [40] N. Lee, W. Choi, P. Vernaza, C. B. Choy, P. H. Torr, and M. Chandraker, "DESIRE: Distant Future Prediction in Dynamic Scenes with Interacting Agents," in *Proceedings of the IEEE Conference on Computer Vision and Pattern Recognition*, 2017.
- [41] X. Mo, Y. Xing, and C. Lv, "ReCoG: A Deep Learning Framework with Heterogeneous Graph for Interaction-Aware Trajectory Prediction," *arXiv preprint arXiv:2012.05032*, 2020.
- [42] F. Poggendorf, J.-H. Pauls, J. Janosovits, S. Orf, M. Naumann, F. Kuhnt, and M. Mayr, "Lanelet2: A High-Definition Map Framework for the Future of Automated Driving," in *2018 21st International Conference on Intelligent Transportation Systems (ITSC)*. IEEE, 2018.
- [43] A. Paszke, S. Gross, F. Massa, A. Lerer, J. Bradbury, G. Chanan, T. Killeen, Z. Lin, N. Gimelshein, L. Antiga *et al.*, "PyTorch: An Imperative Style, High-Performance Deep Learning Library," *arXiv preprint arXiv:1912.01703*, 2019.
- [44] D. P. Kingma and J. Ba, "Adam: A Method for Stochastic Optimization," *arXiv preprint arXiv:1412.6980*, 2014.